



HAL
open science

Modern Southern Junggar Foreland Basin System Adjacent to the Northern Tian Shan, Northwestern China

Chao Li, Shengli Wang, Yanjun Wang, Zhiyuan He, Dongtao Wei, Dong Jia,
Yan Chen, Guohui Chen, Fei Xue, Yunjian Li

► **To cite this version:**

Chao Li, Shengli Wang, Yanjun Wang, Zhiyuan He, Dongtao Wei, et al.. Modern Southern Junggar Foreland Basin System Adjacent to the Northern Tian Shan, Northwestern China. *Lithosphere*, 2022, 2022 (1), 10.2113/2022/7872549 . insu-03671192

HAL Id: insu-03671192

<https://insu.hal.science/insu-03671192v1>

Submitted on 18 May 2022

HAL is a multi-disciplinary open access archive for the deposit and dissemination of scientific research documents, whether they are published or not. The documents may come from teaching and research institutions in France or abroad, or from public or private research centers.







L'archive ouverte pluridisciplinaire **HAL**, est destinée au dépôt et à la diffusion de documents scientifiques de niveau recherche, publiés ou non, émanant des établissements d'enseignement et de recherche français ou étrangers, des laboratoires publics ou privés.



Distributed under a Creative Commons Attribution 4.0 International License

Research Article

Modern Southern Junggar Foreland Basin System Adjacent to the Northern Tian Shan, Northwestern China

Chao Li ¹, Shengli Wang ², Yanjun Wang,³ Zhiyuan He ⁴, Dongtao Wei,⁵ Dong Jia,² Yan Chen,⁶ Guohui Chen ¹, Fei Xue ¹ and Yunjian Li ¹

¹School of Earth Sciences and Engineering, Hohai University, Nanjing 211100, China

²Institute of Continental Geodynamics, School of Earth Sciences and Engineering, Nanjing University, Nanjing 210023, China

³Key Laboratory of Reservoir Characterization, Research Institute of Petroleum Exploration and Development—Northwest, China National Petroleum Corporation, Lanzhou 730020, China

⁴Laboratory for Mineralogy and Petrology, Department of Geology, Ghent University, Krijgslaan 281 S8, 9000 Ghent, Belgium

⁵Xi'an Center of China Geological Survey, Xi'an 710054, China

⁶Univ. Orléans, CNRS, BRGM, ISTO, UMR 7327, F-45071 Orléans, France

Correspondence should be addressed to Chao Li; lichao2019@hhu.edu.cn

Received 3 March 2022; Accepted 29 April 2022; Published 17 May 2022

Academic Editor: Min-Te Chen

Copyright © 2022 Chao Li et al. Exclusive Licensee GeoScienceWorld. Distributed under a Creative Commons Attribution License (CC BY 4.0).

Building-up of the modern Tian Shan range due to the India-Eurasia collision induces the flexural subsidence of the southern Junggar block. The sedimentary infill and subsidence in the southern Junggar foreland basin recorded the growth of the northern Tian Shan. We analyze four seismic profiles, well logging data, and trends in stream morphology in the foreland basin to decipher its architecture, and stratigraphic and subsidence history. The southern Junggar foreland basin system can be divided into the northern Tian Shan wedge-top, Lakes Aiby-Fangcao-Baijiahai foredeep and Luliang forebulge and backbulge depozones. The seismic profiles present the active shortening structures in the wedge top and the northward thinning and onlapping Neogene-Quaternary foreland sequence in the foredeep. The growth strata and unconformities separating the growth and pre-growth strata in the upper part of the foreland sequence are identified in the wedge top depozone. This indicates that the competition between active local folding relief and regional bedrock subsidence determines erosion versus deposition in the wedge top. The logging data of well GQ2 reveal that the present wedge-top depozone evolved from distal lake sedimentation, probably in a foredeep setting, to a braided river in a modern piedmont setting. These lines of sedimentary evidence and the active shortening structures reveal the northward migration process of the southern Junggar foreland basin driven by the northward propagation of the Tian Shan since the Neogene. The north-northeast dipping topography of the northern Tian Shan thrust wedge controls the north-northeastward flowing of all the rivers in the wedge top, and these rivers' flowing direction changes in the foredeep depozone where the tectonic landform flatten out. Growth of anticlines in the front of the wedge-top depozone may have triggered a northward migration of the meandering channel of the Manas river in its lower reach. The transition between the trends of the stream morphology in the wedge top and foredeep depozones suggests the control of the structures of the foreland basin system on trends in stream morphology.

1. Introduction

The modern Tian Shan extending east-west from western China to Kazakhstan is the symbol of neotectonics in Central Asia due to the ongoing collision between the India plate and Eurasian continent during the Cenozoic [1–4]. Relief generation and orogenic erosion related to Cenozoic

shortening and uplifting within the northern Tian Shan range (northwestern China) are responsible for subsidence and the formation of thick fluvial, alluvial, and lacustrine sediments in the southern Junggar basin on the northern flank of the range (Figure 1) [5–7]. Sediments sourcing from the Tian Shan were accumulated in the Junggar Basin, especially in its foreland [7]. The topographic evolution of the

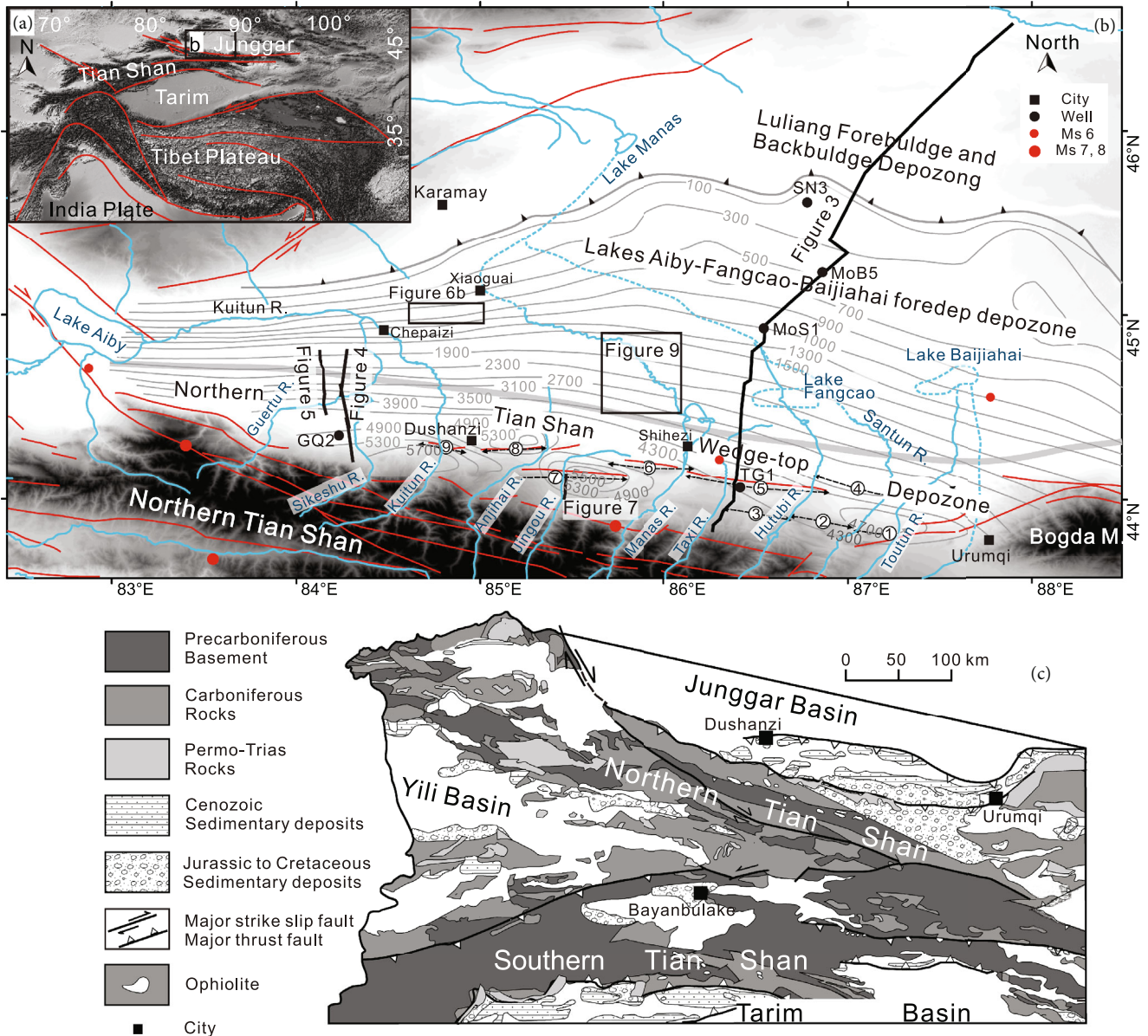


FIGURE 1: (a) Index map showing locus of the modern southern Junggar foreland basin system in framework of the India-Eurasia collision system. Inset square represents Figure 1(b). (b) Shaded relief map of the foreland of the northern Tian Shan showing topographic features, major drainage system, and contours of the thickness from the Neogene to the Quaternary. Contours are based on Song [22] with unit in meter. The gray bold thick line represents the approximate frontier of the southern Junggar foreland fold-and-thrust belt. The black bold line with triangles represents pinching out limit of the Neogene and Quaternary series. Locations of Figures 3, 4, 5, and 7 are marked by the thin black lines. 1-Kalazha anticline, 2-Changji anticline, 3-Qigu anticline, 4-Hutubi anticline, 5-Tugulu anticline, 6-Manasi anticline, 7-Huoerguosi anticline, 8-Anjihai anticline, and 9-Dushanzi anticline. (c) Geological map of the western part of the Chinese Tian Shan (after Charreau et al. [13]).

orogenic range and the subsidence of the coupled foreland basin are linked by the thickened crustal wedge and the surface redistribution of mass due to the erosion of mountain catchments and the sedimentation in foreland basins [8, 9]. Therefore, the sedimentary infill of the southern Junggar foreland basin provides a significant insight into the growth of the northern Tian Shan range through geological time. Recent works used the sediment thicknesses and sedimentation rates of limited section(s) in the foreland basin to reconstruct the shortening and uplifting history of the Cenozoic

Tian Shan (e.g., [10–17]). Changes in the sedimentation rates and the sedimentary environment in the limited section(s) are classically interpreted in terms of changes of regional tectonics or climate (e.g., [10, 13–15, 17]). However, lateral migration of the foreland strata between depozones in the foreland basin, such as wedge-top, foredeep, forebulge, and backbulge depozones, could also cause the similar changes, due to their different structural and stratigraphic characters [8, 9, 18]. This process was often neglected in previous work in this region due to the lack of a comprehensive

study on the division of depozones of the southern Junggar foreland basin system and identification of their structural and stratigraphic characters.

In recent years, numerous high-quality seismic profiles have been acquired during hydrocarbon exploration in the southern Junggar foreland basin, offering an opportunity to decipher its architectures and better understand the foreland dynamics. Magnetostratigraphic studies in the southern Junggar foreland fold-and-thrust belt (e.g., [12–17]) provide reliable chronostratigraphic constraints on the foreland strata. However, the studied sections including pre-growth and growth strata cannot represent real regional sedimentation thicknesses and rates, because growth strata become thinner on the top and limb of growth folds [19]. The fault-related folding theory can help to construct the relation between thicknesses of the top, two limbs of the anticline and synclinal trough (e.g., [19–21]). Seismic data allow us to study the kinematic relation of folds and thrust and to reveal the real sedimentation thicknesses and rates in the southern Junggar foreland.

In this study, we present four north-south trending seismic profiles across the modern southern Junggar foreland basin, together with well logging data which reflect the structure and regional distribution of the late Cenozoic foreland sequence in the foreland basin system. We divide the foreland basin system into three depozones and identify their structural and stratigraphic characters based on the seismic data. The stream morphology trends are also integrated, with the aims of deciphering the architecture and subsidence history of the foreland basin and its implications for the growth of the Tian Shan.

2. Geological Background

Sandwiched between the Tarim craton and the Junggar block, the east-west striking modern Tian Shan range (Figure 1(a)) originated from the accretion and collision of several continental blocks, island arcs, and accretionary complexes in the Paleozoic (Figure 1(c)) [23–25]. This range was reactivated in the Mesozoic in response to major accretion-collision events along the southern Eurasian margin, as attested by previous thermochronological studies (e.g., [26–31]) and sedimentary deposits in the foreland area [5]. It is generally accepted that the present-day topography of the Tian Shan is the result of the stress propagation due to the northward progress and indentation of India into Eurasia [1, 2, 32–36], as supported by obvious crustal shortening in both the Himalayan-Tibetan orogen and Central Asia through GPS measurements (e.g., [37, 38]).

Topographic growth of the Tian Shan range induced flexural subsidence in the foreland basins on its both sides [39–41]. On its northern side, the Paleozoic Tian Shan crystalline basement thrust northward onto the Junggar block. It resulted in the subsidence in the southern Junggar foreland, which accommodates ~5,000 m thick Cenozoic sediments (Figure 1(b)) to form the modern southern Junggar foreland basin system [7, 39, 42, 43].

The active fold-and-thrust belt at the southern margin of the southern Junggar foreland basin accommodated the

crustal shortening between the northern Tian Shan and the Junggar block (Figure 1) [44], with frequent earthquakes (Figure 1(b)) [40]. The timing of initial deformation in the thrust belt is still controversial, ranging from Oligocene (e.g., [45, 46]) to early-middle Miocene (e.g., [13, 47, 48]). The geometry and kinematics of the eastern segment of the thrust belt (on the east of ~85°E) have been well studied (e.g., [17, 41, 44, 49, 50]), but those of the western segment are still poorly investigated. The eastern segment mainly consists of three (southern, middle, and northern) rows of thrust fault-related folds (Figure 1(b)) [40, 51, 52]. The southern row is mostly situated at the range-front with the Lower Jurassic to Cretaceous strata exposing in fold cores; structural shortening has been transferred toward to the foreland, possibly along the Jurassic and Paleogene detachment layers, forming the middle and northern rows of thrust-related folds [49, 50]. GPS observations reveal that this belt is currently accommodating tectonic shortening at a rate of 4.0 ± 1.4 mm/yr [6].

The strata in the modern southern Junggar foreland basin can be divided into pre- and syn-foreland basin depositions [46]. Although the boundary definition is not well defined, the Shawan Formation and the overlying strata are generally classified as syn-foreland-basin formations, including the Shawan, Taxihe, Dushanzi, and Xiyu Formations in ascending order (Figure 2). The Paleogene and the underlying strata were deposited prior to the formation of the foreland basin system. The stratigraphy of the studied zone is detailed in Figure 2.

The Mesozoic sediments are mainly exposed in the fold-and-thrust belt of the southern Junggar foreland basin (Figure 1). From the base upwards, the Jurassic sediments comprise (1) the Lower Jurassic Badaowan and Sangonghe Formations, (2) the Middle Jurassic Xishanyao and Toutunhe Formations, and (3) the Upper Jurassic Qigu and Kalazha Formations. The Cretaceous succession is divided into the Lower Cretaceous Tugulu Group and the Upper Cretaceous Donggou Formation. The Mesozoic sediments has a total thickness of ~1–5 km and contains lacustrine mudstone, siltstone, sandy mudstone, as well as alluvial sandstone and sandy conglomerate.

The Paleogene strata are subdivided into two formations, i.e., the Ziniqanzi and Anjihaihe Formations. The Ziniqanzi Formation, ~150–400 m thick, is dominated by gray-brown pebbly sandstone, gritstone, and fine-grained sandstone. The Anjihaihe Formation, ~130–780 m thick, predominantly consists of brown to grayish siltstone, mudstone, and sandy mudstone.

The Neogene and Quaternary lithologies are made up of four formations: the Shawan, Taxihe, Dushanzi, and Xiyu Formations, which are defined at cliff sections [42] of river valleys in the southern Junggar fold-and-thrust belt. Magnetostratigraphic investigations indicate that the formation boundary ages are diachronous in different sections [12–17]. Specifically, the Shawan Formation, ~150–500 m thick, mainly comprises brownish red sandy mudstone, together with intercalated red to green sandstone, conglomerate and agglomerate limestone. The Taxihe Formation, up to ~330 m thick, includes grayish green mudstone, sandy

Age		Formation	Paleomagnetic age	
Period	Epoch			
Neogene - Quaternary	Plio-Holocene	Xiyu Fm.	~2.1–7.5 Ma	
		Dushanzi Fm.		
	Miocene	Taxihe Fm.	~16 Ma	
		Shawan Fm.	~20.1 Ma	
Paleogene	Oligocene	Anjihaihe Fm.	65.5 ± 0.3 Ma	
	Eocene			
	Paleocene	Ziniquanzi Fm.		
Cretaceous	Upper	Donggou Fm.	145.5 ± 4.0 Ma	
	Lower	Tugulu Group		Lianmuqin Fm.
				Shengjinkou Fm.
				Hutubihe Fm.
				Qingshuihe Fm.
Jurassic	Upper	Kalazha Fm.	145.5 ± 4.0 Ma	
		Qigu Fm.		
	Middle	Toutunhe Fm.		
		Xishanyao Fm.		
	Lower	Sangonghe Fm.		
Badaowan Fm.				

FIGURE 2: Simplified stratigraphic chart of the southern Junggar foreland basin system. The Shawan, Taxihe, Dushanzi, and Xiyu Formations were deposited during the development of the southern Junggar basin system. The paleomagnetic ages are from Charreau et al. [12, 13] and Lu et al. [16]. Note that the same formations may have different lithological characters due to that deposition environments of different depozones are different in the foreland basin system.

mudstone, shell limestone, and marlstone. The Dushanzi Formation, ~200–1300 m thick, consists of fluvial and braided alluvial, brownish-yellow sandy mudstone and sandstone with intercalated grayish green conglomerate. The Xiyu Formation, ~1200–2470 m thick, is predominated by gray sandy conglomerates. The thick late Cenozoic succession was syn-deposited with the development of the southern Junggar foreland basin system. The preserved sediments are distributed northeast-eastwards, with three depocenters located near the Dushanzi (~5700 m), Shanwan (~5500 m), and Changji cities (~4500 m) (Figure 1(b)). The thickness of these lithologies gradually decreases northwards from the depocenters to the Gurbantungut Desert interior which pinch out in the northern margin of the foreland.

3. Interpretation of Seismic Profiles

3.1. Long Seismic Profile across the Junggar Basin. The two-dimensional (2-D) seismic profiles across the southern Junggar foreland basin and well logging data near the profiles were acquired by Xinjiang Oilfield Company, China National Petroleum Corporation. The dominant frequency of the seismic data is 28 Hz, and theoretical vertical seismic

resolution or one-quarter wavelength for the 28 Hz wavelet is ~18 ms (<45 m) in travel time.

A ~326-km-long and 6-second-deep SSW-NNE trending seismic profile across the southern Junggar foreland basin is presented in Figure 3. The long seismic profile was constructed by combining different 2-D seismic profiles across the basin. The boundaries of strata in the seismic profile were determined based on well logging, outcrop data near the profile, and interpretations from previous publications [46, 53–55].

This profile reveals the structure and the regional distribution of late Cenozoic sediments (Figure 3). In the southernmost segment of the profile, the south-dipping thrust faults extend downwards to the Paleozoic and upward to the ground surface. The Meso-Cenozoic strata in this part formed three rows of fault-related folds. The thickness of the Neogene-Quaternary in this part is controlled by the regional structures. In the middle segment, the undeformed Neogene-Quaternary strata gradually thin northward from ~45 km site to ~203 km site in the profile and finally pinch out at ~203 km site (Figure 3). In the northern segment, the basement of the southern Junggar foreland basin system, including Paleozoic, Jurassic, Cretaceous, and Paleogene strata (Figure 2), crops out in the surface. These lithologies are occasionally covered by Holocene thin aeolian bedded sediments, which are <50 m in thickness [42].

Based on the structure and regional distribution of the late Cenozoic sediments illustrated by the seismic profiles (Figures 3–6), we divide the modern southern Junggar foreland basin system into the northern Tian Shan wedge-top, the Lakes Aiby-Fangcao-Baijiahai foredeep, and the Luliang forebulge and backbulge depozones (Figures 1(b) and 3).

3.2. Seismic Profiles in the Wedge Top and Foredeep Depozones. Figure 4 shows a ~68-km-long and ~6.5-second-deep seismic profile crossing the western segment of the northern Tian Shan wedge-top and Lakes Aiby-Fangcao-Baijiahai depozones.

The Tuosite homocline, the Xihu and N-Xihu anticlines, and synclines between them in the wedge-top depozone are well illustrated in the seismic profile (Figure 4). The Tuosite homocline belongs to the front limb of the southernmost fault-bend fold, and the front limb dips northwards with varying dip angles (10–20°). The Tuosite homocline defines the southern boundary of the wedge-top depozone, where the foothills of the Tian Shan range are now undergoing erosion. The foreland sequence that comprises the shallow part of the Tuosite homocline was exposed to the surface by tectonic uplift of the fault-bend folds. The Meso-Cenozoic successions in the region between the Tuosite homocline and the Xihu anticline remain undeformed.

The Xihu anticline is characterized by a detachment fold, with detachment layer situated within the Jurassic Badaowan Formation to the lower part of the Dushanzi Formation, but keeps relative constant from the upper part of the Dushanzi to Xiyu Formations (Figure 4). The Xihu anticline is bilaterally symmetrical, with dip angles descending upwards to approximate horizontal as represented by the

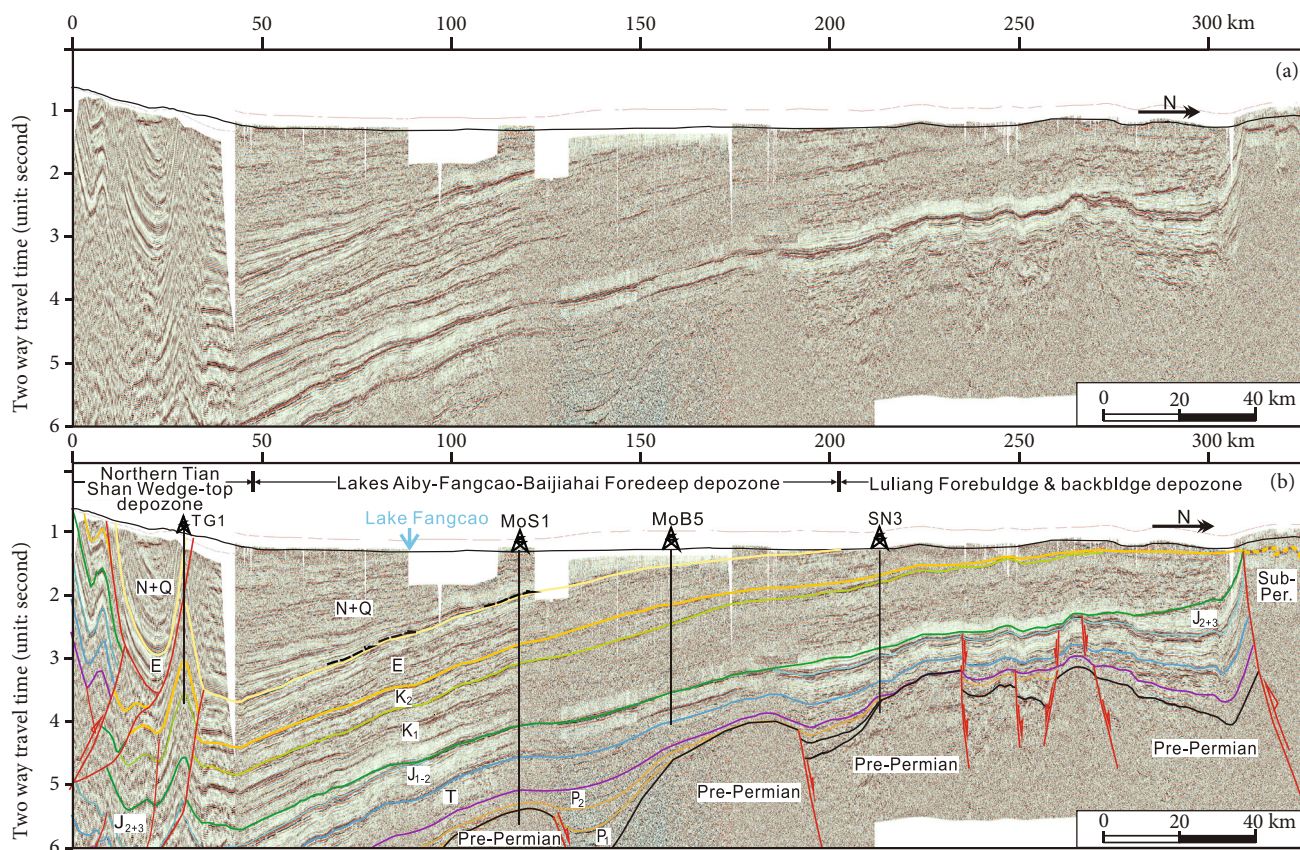


FIGURE 3: Original (a) and interpreted (b) seismic transverse section crossing the southern Junggar foreland basin system, see Figure 1(b) for the location (modified after Wang et al. [54]). The northern Tian Shan wedge-top, Lakes Aiby-Fangcao-Baijiahai foredeep, and Luliang forebulge and backbulge depozones are illustrated. It is difficult to identify the limit between the Luliang forebulge/backbulge depozone and the craton. The black half-arrows represent the late Cenozoic foredeep sequence onlaps forelandward. Vertical exaggeration is about 9X.

top reflectors. These characteristics of geometry of the Xihu anticline is similar to that of the typical detachment folds [20]. Seismic reflectors at the southern limb of the anticline are better defined than those at the northern counterparts, which is likely to be related to the effects of structural barriers of the anticline. Growth of the anticline caused topographic uplift and therefore the formation of structural barriers for sediment dispersal. In the southern limb, low-energy sedimentation produced stratigraphic units with well-defined reflectors. While on the top of the structural barrier, high-energy sedimentation resulted in stratigraphic units without well-defined seismic reflectors. There only exists a shallow river channel (named the Ganhezi stream) that flows through the Tuosite structure and the Xihu anticline, having incised the Xihu anticline to form a cliff of about 50 m high. It is much smaller than the mean incision depth of rivers on the north piedmont of the Tian Shan (~124 m) [56]. This implies that the age of the Xihu anticline could be very young.

The N-Xihu anticline, as the front of the orogenic wedge, is located to the north of the Xihu anticline and interpreted as the distal part of the wedge-top depozone. Likewise, it is a detachment fold, characterized by a smaller folded region and thinner growth strata than the Xihu anticline (Figure 4). This implies a forward propagation of the

northern Tian Shan orogenic wedge. No structure associated with the fold-and-thrust belt is observed on the north of the N-Xihu anticline. The N-Xihu anticline is not well exposed on the surface. Relative surface elevations of the Tuosite structure, the Xihu and N-Xihu anticlines decrease toward to the foreland, which may indicate that their initial growth ages tend to be younger from the south to north.

The seismic profile (Figure 4) shows the foreland sequence tapers forelandward from the north of the N-Xihu anticline. This means that the modern foredeep depozone develops in the north of the N-Xihu anticline (Figures 2 and 4).

Figure 5 shows a ~30 km long and 6-second-deep north-south trending seismic profile in the Lakes Aiby-Fangcao-Baijiahai depozone near Figure 4. The seismic reflectors in the bottom of the Shawan Formation terminate to the north on the top of the Paleogene, revealing the progressive northward onlap of the late Cenozoic foreland sequence in the foredeep depozone (Figure 5).

A short north-south trending seismic profile in the northern part of the Lakes Aiby-Fangcao-Baijiahai foredeep depozone (Figure 6) shows that a series of normal faults developing in the thick late Cenozoic succession. These normal faults reveal small-scaled displacements of less than two seismic reflectors (ca. 12 m). The displacements gradually reduce upwards and disappear in the shallower sequence

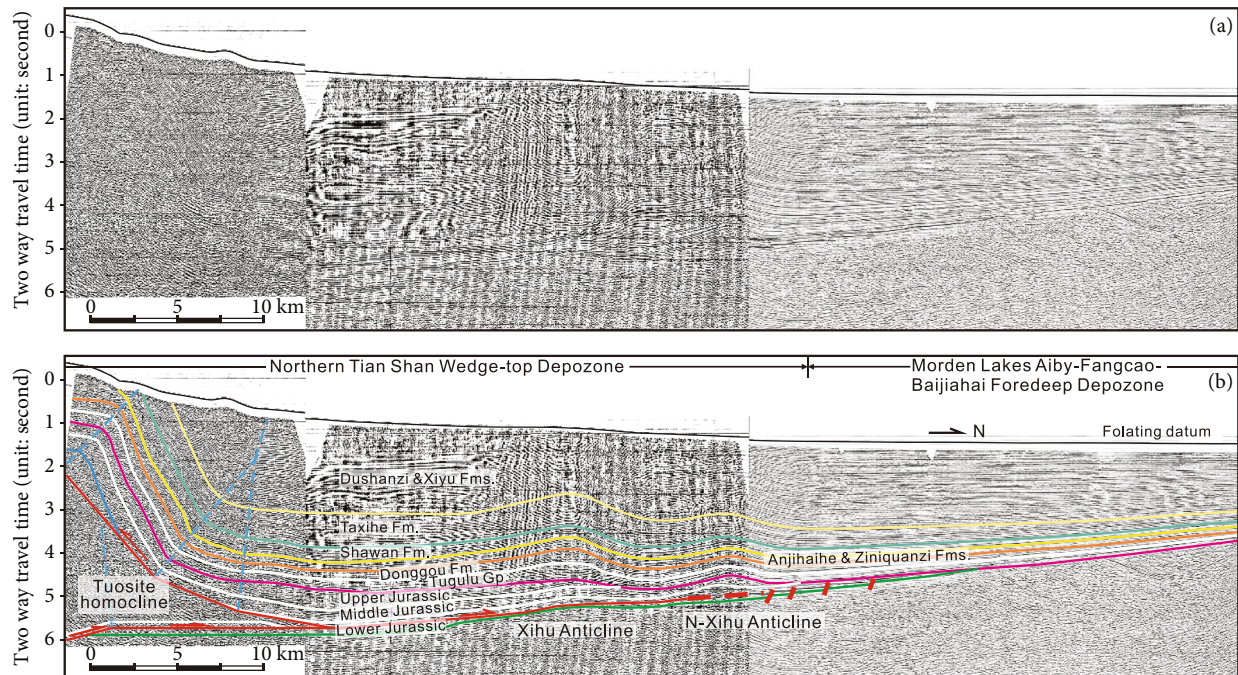


FIGURE 4: Original (a) and interpreted (b) seismic transverse section crossing the west segment of the southern Junggar foreland basin system, see Figure 1 for the location. The sediments syn-deposited with the development of the southern Junggar foreland basin system taper bilaterally from the north side of the Xihu anticline. The southern side tapering is caused by intensive erosion of the folded strata, whereas the northern counterpart is characterized by a northward progressive tapering due to the flexural subsidence of the southern Junggar basin basement, together with a smaller gradient tendency. The N-Xihu (north Xihu) anticline, the submerged youngest growth structure in the western segment of the foreland basin system, is a detachment fold anticline located to the front of the southern Junggar fold-and-thrust belt.

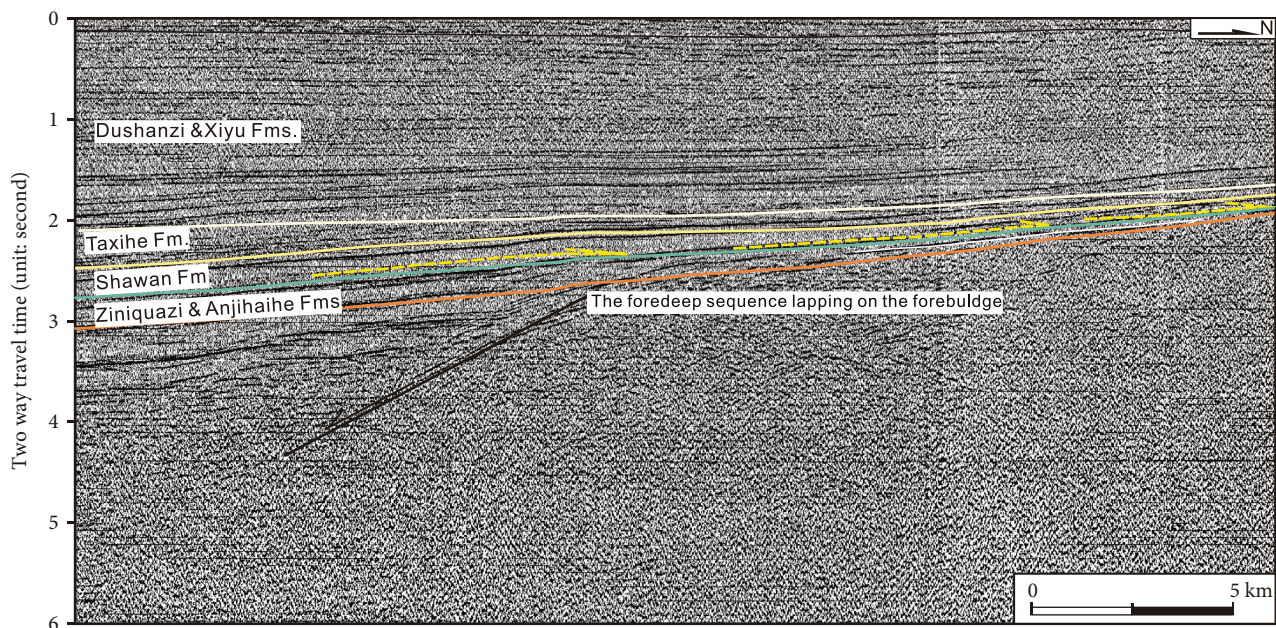


FIGURE 5: Interpreted seismic section across the west segment of the Lakes Aiby-Fangcao-Baijiahai foredeep depozone in the southern Junggar foreland basin system. The yellow half-arrows represent the foredeep sequence onlaps forelandward. See Figure 1 for location.

(Figure 6). Their occurrence indicates that there existed a localized extensional zone in the compressional setting. However, in contractional foreland basin systems, normal

faults are usually restricted to the forebulge zones due to the flexure of the lithosphere [8]. Therefore, the normal faults presented in Figure 6 may represent the ancient

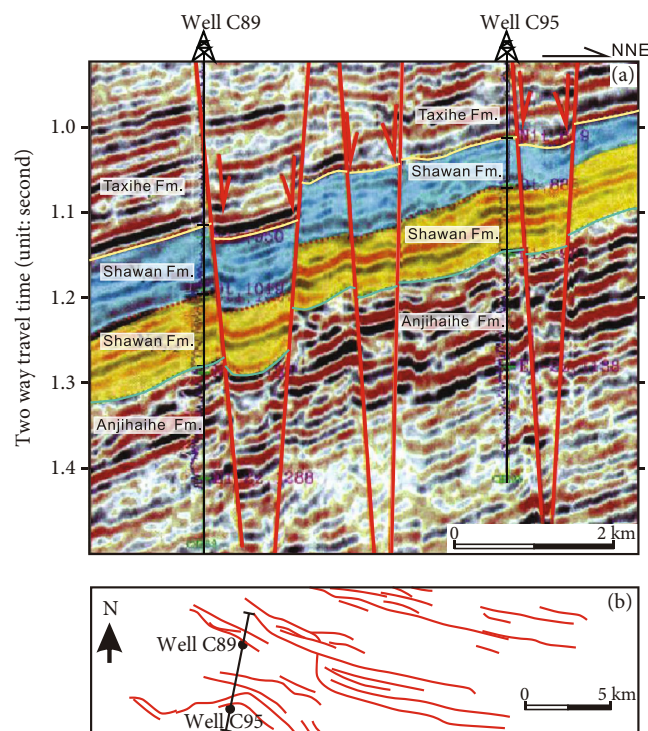


FIGURE 6: Interpreted seismic section in the Lakes Aiby-Fangcao-Baijiahai foredeep depozone that shows the east-west trending normal faults in the late Cenozoic strata, indicating the potential position of the ancient forebulge in the southern Junggar foreland basin system (a) and map distribution of the normal faults in part of the ancient forebulge (b) (modified after Yu et al. [57]).

forebulge of the foreland basin system to the south of the present-day's Luliang forebulge.

The north-south trending seismic profile in Figure 7 crosses the middle segment of the northern Tian Shan wedge-top depozone. This profile shows the structure of the northern limb of the W-Gobi anticline, the Huoerguos anticline, and the deposition features of the synclinal trough in the middle segment of the wedge-top depozone.

The W-Gobi anticline is a fault-bend anticline, and its northern limb to the north of the fixed axial surface is shown in Figure 7. The flat top and partial northern limb of the W-Gobi anticline are eroded to produce the accommodation space for the accumulation of deposits in the syncline to the north. In addition, this resulted in the formation of the unconformity between the pre- and syn-growth strata. In the structural low of the synclinal trough, the unconformity gradually becomes a conformable stratigraphic horizon (Figure 7). The pregrowth and growth strata all dip northwards, but the latter exhibits lower and subhorizontal dip angles, indicating that the topographic slope of the southern limb of the synclinal trough progressively diminishes. Filling of the syncline trough to the north of the W-Gobi anticline is dominated by an ancient slope due to the erosion, instead of the growth of the W-Gobi anticline. The flat top and front limb of the anticline were eroded, it is therefore difficult to retrieve its growth process. There are no observed unconformities in the southern limb of the Huo-

guos anticline. Hence, the northern limb of the W-Gobi anticline and the syncline to the north passively move toward to the foreland. The seismic profile is very close and near parallel to the sampling locations of the magnetostratigraphic column in the well-exposed Jingou river section [13], which constrained the ages of the bottoms of the Shawan, Taxihe, Dushanzi, and Xiyu Formations (Figures 2 and 7). The dip angles of strata from the middle part of the Dushanzi Formation descend southward along the Jingou river section, which are likely to be related to limb rotation [51] or curved kinked band migration [58]. These works indicate that the Huoerguos anticline was active during the Miocene and is still active at the present.

4. Sedimentary Environment Changes in Well-Upward Section

Upsection changes in the depositional setting of strata located in the wedge-top depozone have been widely used to recognize the uplift of the Tian Shan and possible climate change (e.g., [11, 56, 59]). The well data, illustrated in Figure 8, show the changes of vertical sedimentary environment in the well-upward section in the western segment of the wedge top.

The well GQ2 is located in the western segment of the northern Tian Shan wedge-top depozone (Figure 1(b)). The sedimentary sequence starts with the Taxihe Formation (2340-2280 m), passes gradually upwards into the Dushanzi Formation (2284-704 m), and culminates in the Xiyu Formation (704-0 m) (Figure 8). The grain size is generally coarsening upwards from the upper part of the Taxihe Formation, while related water depths of the sedimentary environment indicate a shallowing-upwards tendency; i.e., from lake to seasonal piedmont alluvial fan system. The sedimentary environment characterizes the lacustrine system from 2340 m to ~1600 m deep (the top part of the Taxihe Fm. and the lower part of the Dushanzi Fm.), a gravelly fluvial system with medium-grained floodplains from ~1600 m to ~1100 m deep (the upper part of the Dushanzi Fm.), a gravelly fluvial system with coarse-grained floodplains from ~1100 m to ~410 m deep (the top part of the Dushanzi Fm. and the lower part of the Xiyu Fm.), and a gravelly alluvial fan from ~410 m to surface (the upper part of the Xiyu Fm.). The sedimentary environment changes record the migration process that the position of well GQ2 relative to the Junggar block has involved from the proximal part of the foredeep zone to the northern Tian Shan wedge-top depozone.

5. Trends of Stream Morphology

Morphology and distribution of drainage networks constitute a response of landform to regional tectonic process (i.e., uplift and subsidence) [60, 61]. In the following section, we present the analyses of the trends in the stream morphology across the northern Tian Shan piedmont.

Numerous north-flowing rivers originating from the Quaternary glaciers in the interior of the Tian Shan range [56] exist within the northern Tian Shan wedge-top

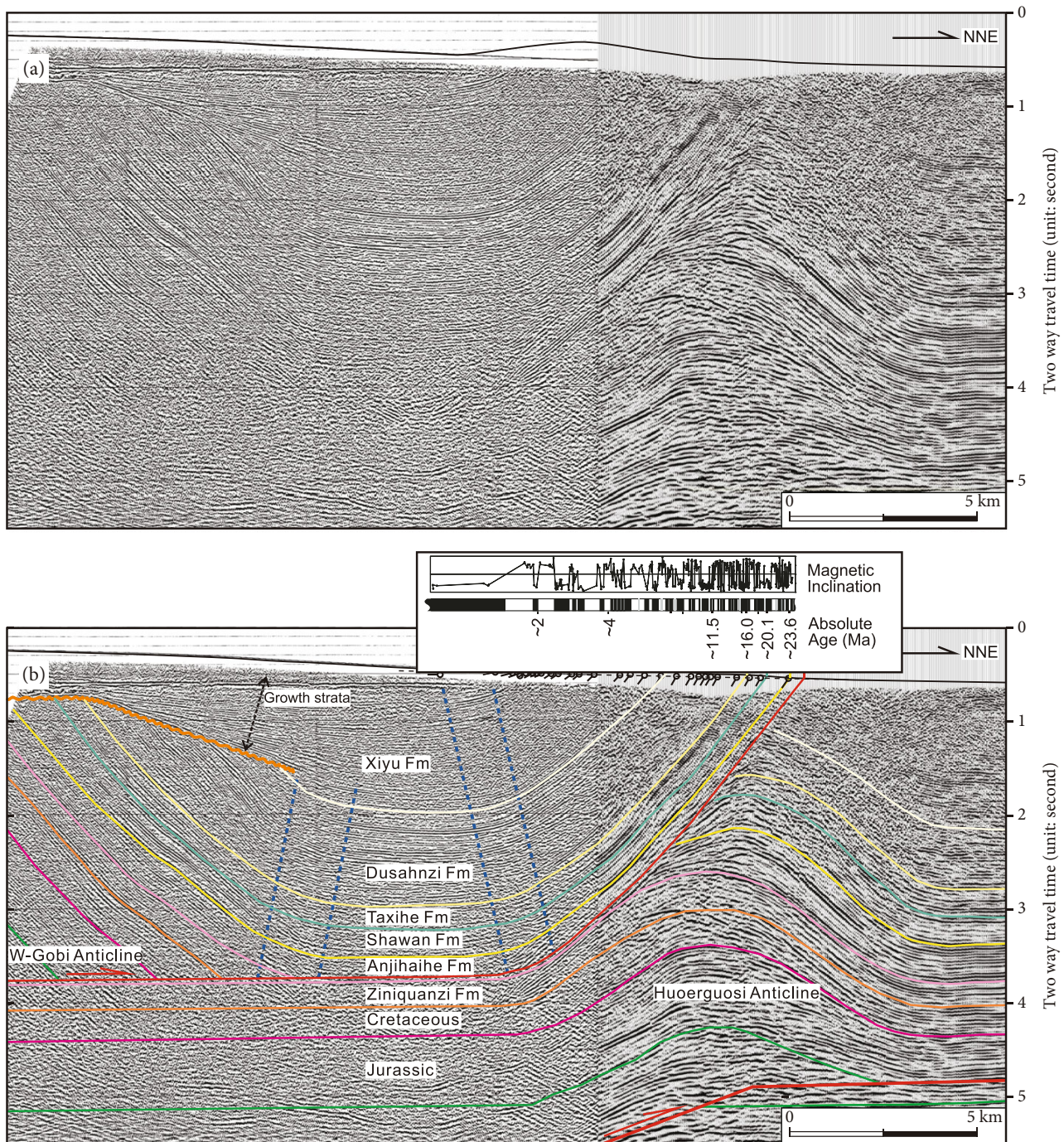


FIGURE 7: Interpreted seismic section across the north limb of the W-Gobi (west Gobi) anticline and the Huoerguosi anticline (modified from Wang et al. [46]). The W-Gobi fault-bend fold anticline is located in the transitional zone between the Tian Shan and the southern Junggar fold-and-thrust belt. In the north limb of the W-Gobi anticline, the pre-growth strata were partly eroded, and the detritus was deposited in the neighboring syncline. A remarkable unconformity (the orange wavy line) exists between the pre-growth and growth strata, which gradually disappears in the core of the syncline and turns to be a conformity or disconformity. Dip angles of the growth strata on the northern limb of the W-Gobi anticline gradually become lower to horizontal, implying that the filling of the syncline trough was mainly controlled by ancient topography. The blue dashed lines are inferred axial planes. See Figure 1 for location. The magnetostratigraphic column is based on Charreau et al. [13].

depozone extending about 220 km long from Urumqi to Kuitun with flowing direction approximately perpendicular to the strike of the Tian Shan range (Figure 1(b)). To be more specific, they are Urumqi, Toutun, Santun, Hutubi,

Taxi, Manas, Ningjia, Jingou, Anjihai, and Kuitun rivers with the intervals among them of ~27 km, ~17 km, ~27 km, ~30 km, ~25 km, ~21 km, ~22 km, ~26 km, and ~30 km, respectively, and an average of $\sim 25 \pm 4$ km. These rivers

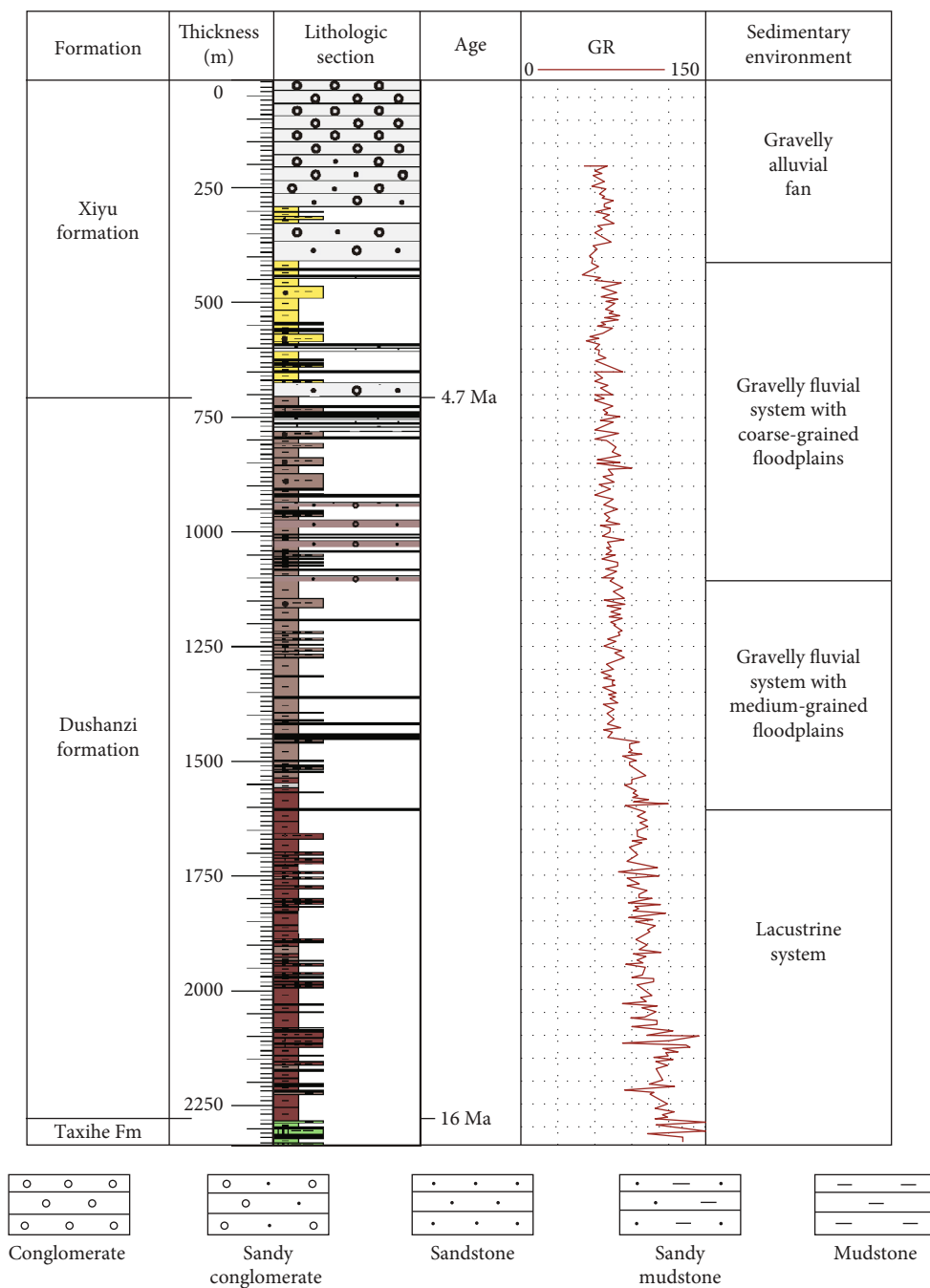


FIGURE 8: Stratigraphy, sedimentary environment, and plot of neutron-gamma radiometer (GR) of well GQ2 in the foredeep depozone near the profile in Figure 4, see Figure 1(b) for location. Sediment grain size indicates a coarsening-upwards sequence from the upper part of the Taxihe Formation, together with a shallowing-upwards tendency of water depths of sedimentary environment (from lake to seasonal piedmont alluvial fan system).

deeply incise the mountain range bedrocks and the foreland basin sediments, creating deep river valleys and well-developed fluvial geomorphic sequences [62–64]. The relatively stable interval length implies that the formation of these rivers was controlled by the north-dipping topographic slope in the wedge-top zone [52, 62].

From the wedge-top depozone to the flood plain, some rivers that flow into tail lakes had been used up for irrigation. This led to localized desiccation as evidenced by the

Manas, Fangcao, and Baijiahai lakes (Figure 1(b)). Similarly, the exceeding cultivation has reshaped meandering river channels in lower reaches and occupied the tail lakes by farmland. We thus have to identify the undisturbed distribution of rivers and tail lakes in lower reaches to understand the relationships between the evolution of the foredeep depozone, river diversion, and formation of lakes. Zhang and Li [65] and Zhang et al. [66] reconstructed the migration of the Manas, Santun, and Hutubi rivers for the last

300 yrs by using the historical maps, the local choreographies of Xinjiang and several counties as well as modern climatology, hydrology, and remote sensing images. Combining these previous works and the present shapes of the rivers, the diversion of these river systems is summarized in the following.

Away from the orogenic wedge, the Urumqi river diverts anticlockwise by $\sim 41^\circ$ from north-north-east to north-north-west; the Toutun river remains its flow direction (Figure 1(b)). Both of them flow into the Baijiahai lake that has dried up as a result of agricultural consumption [66].

In the proximal parts of the foredeep, the Santun river diverts anticlockwise by $\sim 83^\circ$ from north-north-east to northwest (Figure 1(b)). The Hutubi River diverts anticlockwise by $\sim 89^\circ$ from north-north-east to northwest and then flows into the Fangcao lake. The lower reach of the Hutubi river merges with the Santun river to the north of the Fangcao lake. The merged Luokelun river continues to flow northwestwards and then diverts north-north-eastwards at the town of Xiaoguai (Figure 1(b)) and finally flows into the Manas lake [66].

The Manas river, characterized by the widest valley area in the northern piedmont of the Tian Shan, diverts anticlockwise by $\sim 90^\circ$ and flows northwestwards from the city of Shihezi to the town of Xiaoguai (Figure 1(b)). Based on satellite images and field reconnaissance, the present (R4) and 3 abandoned (R3, R2, and R1) meandering channels of the Manas river in its lower reach (Figure 9) are distinguished [67]. More abandoned older river channels reworked by surface process and human activity are, however, difficult to be recognized. The ^{14}C ages of R4, R3, R2, and R1 are 0~500, 500~1500, 1500~4000, and >4000 yrs B.P., respectively [67]. These ages show that the meandering river channels of the Manas river in the lower reach migrated northwards no later than 4000 yrs B.P.

The Taxi river directly flows northwards and merges into the Manas river. The ancient channel of the Jingou river had been occupied by the Anjihai river. The Jingou river flows north-east-eastwards along the south margin of the emergent Anjihai anticline ridge due to its growth, diverts northwards at its eastern plunging end, and then merges into the Manas river. The Anjihai river diverted in the Quaternary, previously abandoned its channel and alluvial fan, and occupied the Jingou river channel at the middle segment of the Anjihai anticline. Flowing through the orogenic wedge, the Anjihai river runs northwards and merges into the Manas river. In the flood plain, the Taxi, Qingshui, Jingou, and Anjihai rivers all merge into the Manas river which flows northwestwards parallel to the Luokelun river. At the town of Xiaoguai, the Manas river diverts northwestward and merges into the Luokelun river, then finally flows into the Manas lake (Figure 1(b)) [65]. In the western margin of the foredeep, the Kuitun river diverts northwestwards and then south-west-westwards again at the Chepaizi town and finally flows into the Aiby lake. The Sikeshu and Guertu rivers are headed from the mountain range and then merge with the Kuitun river (Figure 1(b)).

In summary, the rivers sourcing from the Tian Shan range flow into the Lakes Aiby-Fangcao-Baijiahai foredeep

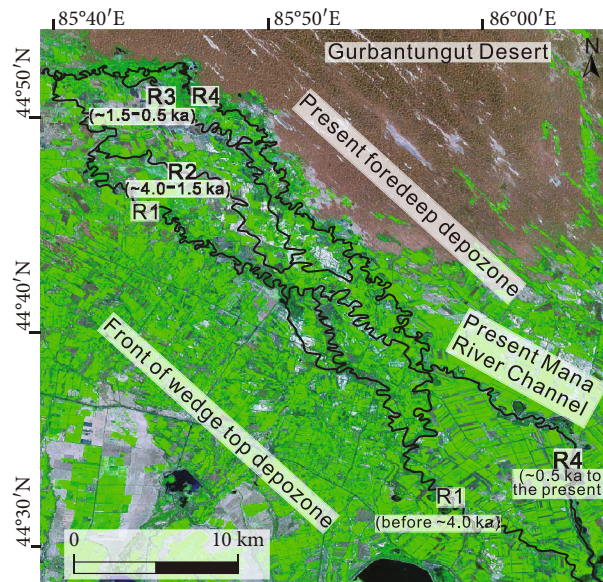


FIGURE 9: The present and ancient abandoned meandering channels of the lower reach of the Manas river to the north of the northern Tian Shan orogenic wedge (modified after Cui et al. [67]). R4—the present meandering channel of the lower reach of the Manas River 500 years ago to the present, R3—the abandoned meandering river channel 1500 to 500 years before present, R2—the abandoned meandering river channel 4000 to 1500 years before present, and R1—the abandoned meandering river channel earlier than 4000 years before present. The ages of the channels show that the meandering channels of the Manas River in its lower reach migrated northwards since earlier than 4000 years before present.

depozone and then divert to the direction parallel or subparallel to the range and finally flow into the tail lakes of Aiby, Manas, Fangcao, and Baijiahai. Except for the lake Manas, the lakes Aiby, Fangcao, and Baijiahai are arrayed, and the river channels parallel to the range are located between them (Figure 1(b)). The locations of the tail Lakes Aiby, Fangcao, and Baijiahai represent the present depocenter in the foredeep zone (Figures 1 and 9), which is located ~ 40 km to the north of the depocenter of the late Cenozoic foreland sequence (Figure 3). The tail north-north-east segment of the Manas river channel is inferred to be located in the forebulge depozone. The lake Manas is beyond the southern Junggar foreland system.

6. Discussion

With the architectures of the southern Junggar foreland basin system revealed by the seismic profiles, we divide the modern southern Junggar foreland basin system into the northern Tian Shan wedge-top, the Lakes Aiby-Fangcao-Baijiahai foredeep, and the Luliang forebulge and backbulge depozones based on the present tectonics, subsidence, and drainage system in the basin.

6.1. Division of Depozones of the Foreland Basin System. Our interpretation of the seismic profiles across the southern

Junggar foreland basin (Figures 3–7) reveals the characteristics of the structure, subsidence, and regional foreland sequence distribution of the northern Tian Shan wedge-top, the Lakes Aiby-Fangcao-Baijiahai foredeep, and the Luliang forebulge and backbulge depozones (Figures 10 and 11).

In the northern Tian Shan wedge-top depozone, the growth strata and unconformities that separate the pre-growth and growth strata are identified in the upper part of the fault-related folds based on the seismic profiles (Figure 7), suggesting local folding relief and regional bedrock subsidence resulted from the uplift and shortening of the adjacent orogen [19, 68, 69]. Their competition determines erosion versus deposition in this area during the development of the foreland basin. If the amplitude of local folding relief is greater than regional subsidence, the erosion of the thrust belt predominates. In contrary, if the amplitude of regional subsidence is greater than local folding relief, the deposition occurs. For example, in the structural low of the syncline between the W-Gobi and Huoerguos anticlines, the growth strata exhibit lower and subhorizontal dip angles than the pre-growth ones (Figure 7), indicating that the amplitude of regional subsidence was greater than local folding relief, and the filling of the syncline trough was dominated by the ancient slope. The growth strata in the upper part of the foreland sequence are also found in the area between the first and second rows of anticlines in the eastern segment of the thrust belt [51]. It is comparable with those strata in the syncline between the W-Gobi and Huoerguos anticlines in the middle segment (Figure 7). Hence, the competition between active local folding relief and regional bedrock subsidence determines the erosion versus deposition of sediments in the wedge top depozone.

The thickness of the late Cenozoic growth strata in the northern Tian Shan wedge-top depozone is dominated by the fault-related folding [13, 58]. The thickness of the growth strata on the structural high is thinner than that on the structural low. In some cases, the absence of growth strata in the structural high causes the formation of unconformity. Accordingly, the stratigraphic thickness on the fold limb cannot always represent sediment accumulation in a wedge-top depozone, but the sediments accumulated in a syncline could work. Local folding effects on sediment thickness should be taken into account when calculating sedimentation rates in wedge-top depozones [68, 69]. The sediment thicknesses in the syncline can be extrapolated according to geometry and kinematics of folding based on seismic data and surface geology, and the thickness of growth strata on the anticline limb should be calibrated to the thickness on the neighboring syncline adapting a suitable folding model [69]. Therefore, regarding the analyses on the river sections, long-term subsidence characteristics of the foreland basin system and effects of the local fold should be carefully considered, when deducing the uplift process of the Tian Shan range (e.g., [12–17]).

Previous field mapping and seismic data indicate that there are three rows of anticlines in the eastern segment of the depozone: the Qigu-Changji-Kalazha, Huoerguos-Manas-Tugulu, and Hutubi-Anjihai-Dushanzi anticline

zones from south to north (Figure 1(b)) [44, 48–50, 70]. Our new seismic data reveal that there also exist a row of subsurface anticline structures to the north of the Hutubi-Anjihai-Dushanzi anticline zone, named the N-Xihu–N-Dushanzi–W-Hutubi–N-Hutubi anticline zone in the western segment of the wedge top zone (Figures 3 and 4). The sequences at the front of the third row of the anticlines in the eastern segment are comparable to those in the Xihu and N-Xihu anticlines in the western segment (Figure 4).

The Lakes Aiby-Fangcao-Baijiahai foredeep depozone with a width of ~160 km (Figure 3) form the main part of the southern Junggar foreland basin system and accommodate the sediments sourced from the Tian Shan range. The foreland sequences in the foredeep are characterized by the trend of gradually northward thinning and onlapping from its proximal to distal parts (Figures 3 and 4).

The Luliang forebulge and backbulge depozone are characterized by the outcropped basement of the foreland basin, including Paleozoic, Jurassic, Cretaceous, and Paleogene strata; they are occasionally covered by Holocene thin aeolian bedded sediments in the Gurbantungut Desert [42].

6.2. Implications for the Growth of the Northern Tian Shan.

In an orogenic wedge-foreland basin system, the propagation of the orogenic wedge drives the forelandward migration of the coupled foreland basin as well as sedimentary facies by inducing the flexure of the lithosphere (e.g., [18, 71–73]). The shortening structures in the southern Junggar foreland fold-and-thrust belt indicate the northward propagation of the northern Tian Shan orogenic wedge since the late Oligocene [2, 13, 44, 46], but the migration of the southern Junggar foreland basin is not well documented. We provide new evidence for the forelandward migration history of the modern Junggar foreland basin system by presenting seismic profiles crossing the foreland basin and well data within it and integrating the trend in the stream morphology (Figure 11).

The progressive northward onlaps of the late Cenozoic foreland sequence are identified in the seismic profiles crossing the foredeep depozone (Figures 4 and 5). In foreland units, the trace of the forelandward onlap points represents the forelandward displacement of the forebulges [74–76]. The oldest sedimentary sequence in the southern Junggar foreland basin is of the Shawan Formation deposited since ~24 Ma based on magnetostratigraphic constraints [13, 46]. Hence, the progressive northward onlaps of the foreland sequence demonstrate the northward migration of the southern Junggar foreland basin since ~24 Ma and record the filling history of the basin. Furthermore, the migration of the forebulges is also revealed by the possible ancient forebulge with numerous normal faults in the distal part of the present foredeep (Figure 6).

In the process of the forelandward migration of foreland basin systems, the site in the underthrust plate would experience the evolution of depozones in the foreland basin system from the distal end to the proximal end, until being involved in the orogen [77]. This process was recorded by the sediments above this site from the bottom to surface in classical foreland basins, such as the Ganga foreland basin

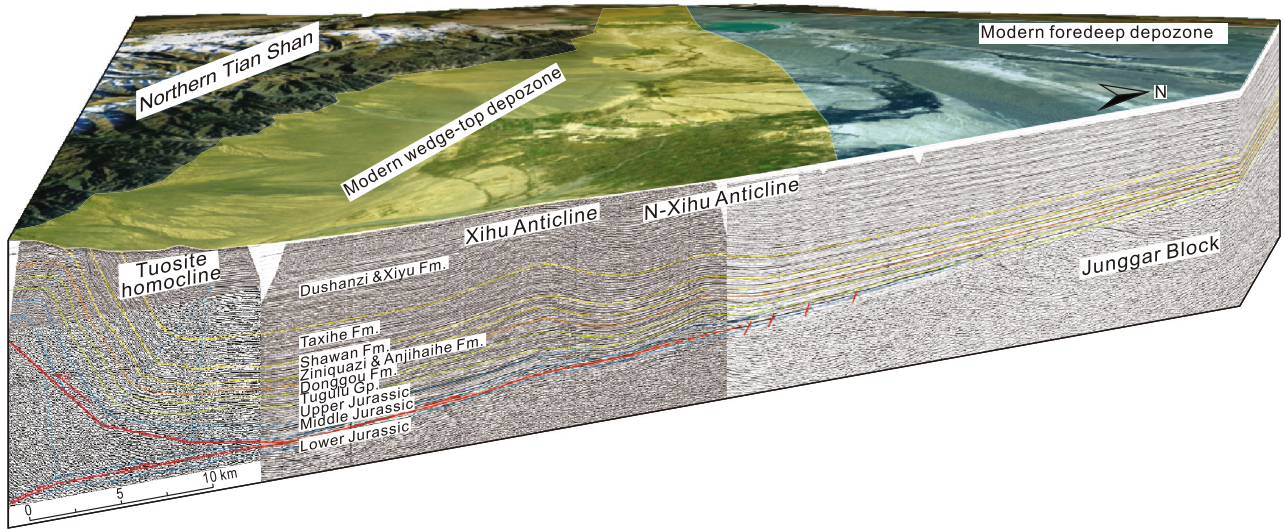


FIGURE 10: Block diagram showing the Tian Shan thrust over Junggar, resulting in the subsidence of the southern Junggar and forelandward growth of the fold-and-thrust belt.

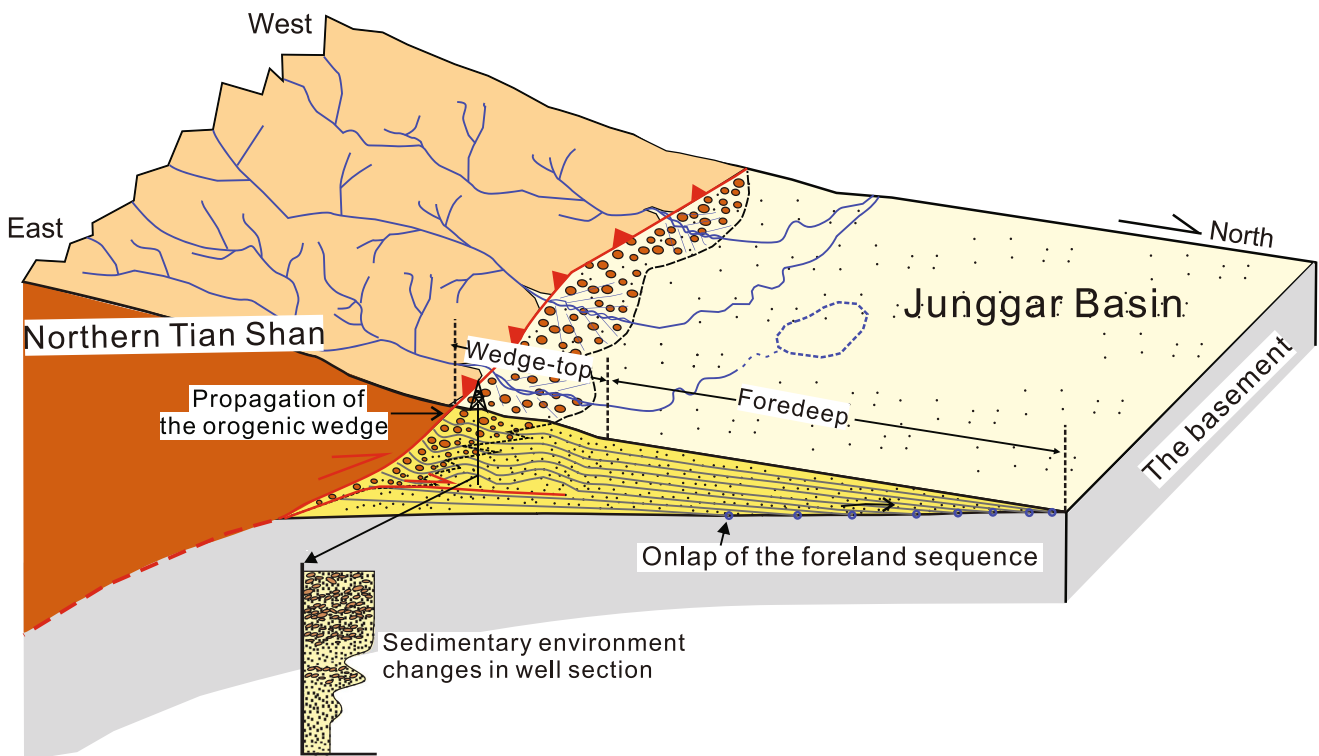


FIGURE 11: Schematic sketch of the modern southern Junggar foreland basin system shows the relationship between the subsurface structure of the foreland sequence and the trends in stream morphology in the basin. The northward onlaps of the foreland sequence and the sedimentary environment changes in vertical sections reveal the forelandward migration of the foreland basin.

[18, 78], the North Alpine foreland basin [79], and the western Taiwan foreland basin [80]. In the terrigenous foreland basin system, sedimentary environments above the site changes regularly through shallow to deep water until the piedmont alluvial system [18]. This evolutionary tendency can be found in the vertical sections in the southern Junggar

foreland basin system. The vertical sedimentary environment changes in well GQ2 from lacustrine to seasonal piedmont alluvial fan system imply that the site of well GQ2 has undergone from the proximal part of the foredeep zone to the northern Tian Shan wedge-top depozone. The foreland basin sequences in the Jingou river section [13] in

the middle segment of the wedge top above the Taxihe Formation show a similar change tendency in sedimentary environment with respect to well GQ2. In the Jingou river section, the exposed Cenozoic strata of ~4400 m thickness are classified into 12 sedimentary units (see Figure 12 in Charreau et al. [13]). The sediment grains above the Taxihe Formation become coarse upwards, and water depths of sedimentary environment become shallow from lake to seasonal piedmont alluvial fan system. It also reveals the migration process of a site in the present-day northern Tianshan wedge top, from distal part of the foredeep depozone to proximal part, until to the wedge-top depozone. Therefore, the vertical sedimentary environment changes revealed by well GQ2 and the Jingou section can be considered as footprints of forelandward migration of the southern Junggar basin system.

Gravity anomaly indicates that the Tian Shan range between the Tarim and the Junggar blocks is in Airy equilibrium, and the regional compensation occurs on the range [81, 82]. Therefore, the topographic growth of the Tian Shan range and the subsidence of the southern Junggar foreland basin are coupled. The changes in sedimentation rates in the sites in the southern Junggar foreland were used to reconstruct the uplifting history of the Cenozoic Tian Shan (e.g., [11, 13, 16]). However, the migrating process from the proximal part of the foredeep depozone to the wedge top depozone could also be responsible for changes in sedimentation rates of the foreland sequence in the wedge top depozone (Figure 11).

Charreau et al. [13] constructed the sediment accumulation curve of the southern Junggar foreland basin system along the Jingou section since ~23.6 Ma. They interpreted the two increases in the sediment accumulation rates at ~16–15 Ma and ~11–10 Ma as two pulses of enhanced uplift of the Tian Shan. Nevertheless, in the framework of the southern Junggar foreland basin system, the sediment accumulation curve is comparable to the typical sediment accumulation curve of the foreland basin system. The two increases in the curve could represent that the site of the Jingou river section gradually migrate into the foredeep depozone in the period from ~15 Ma to ~10 Ma. The relative constant sedimentation rate from ~10 Ma to ~4 Ma indicates that the site of the Jingou river stayed in the foredeep. Whereas the decrease in the sedimentation rates at ~4 Ma could demonstrate the site migrated into the wedge-top depozone, which is close to the boundary age of the pre-growth and growth strata at the southern limb of the Huoerguos anticline, ~4 Ma, based on the correlation between the seismic profile and magnetostratigraphic section [51, 58], slightly earlier than that of the Anjihai anticline to the north [83].

6.3. Tectonic Impacts on Trends of Stream Morphology. We analyzed the trends in stream morphology across the Junggar foreland. The north-northeast dipping topography of the Tian Shan orogenic wedge controls the north-northeastward flowing of all the rivers in the wedge top [62, 63], but they divert to the direction parallel or subparallel to the range in the foredeep depozone where the tectonic landform due to the active thrust belt flatten out (Figures 3

and 4) [52, 63, 84]. The transition between the trends of the surface stream morphology in the wedge top and foredeep suggests the control of the subsurface structures of the foreland basin system on trends in the stream morphology (Figures 10 and 11).

The meandering river channel in the lower reach of the Manas river is migrating northwards in the transitional zone between the wedge-top and the foredeep (Figure 9) [67]. The northward propagation of the northern Tian Shan orogenic wedge triggers the northward growth of the frontier fold and increases the surface slope to lead to river diversion/channel migration. Although the sudden river diversion is often ascribed to a catastrophic flood event, several migration events to the same direction imply that the migration tendency is dominated by one intrinsic factor (e.g., [61]). The thrust faults beneath the Manas river in the southern Junggar thrust-and-fold belt is still active at 10^3 year-time scale with two important registered earthquakes of $M_s > 6$ (Figure 1(b)). Hence, we attribute the migration of the Manas meandering river channel to the increment of the north-dipping slope due to the northward propagation of the thrust-and-fold belt (Figure 1(b)) [40]. The evolution of the Manas river channels in the last 4 ka (Figure 9) may suggest that the migration of the drainage system in the basin was driven by the topographic growth of the northern Tian Shan wedge.

7. Conclusions

- (1) The modern southern Junggar foreland basin system can be divided into the northern Tian Shan wedge-top, Lakes Aiby-Fangcao-Baijiahai foredeep, and Luliang forebulge and backbulge depozones. The propagation of the northern Tian Shan range has been driving the northward migration of the southern Junggar foreland basin, together with sedimentary facies since the Neogene
- (2) The competition between local folding relief and regional bedrock subsidence determines the erosion versus deposition in the wedge top depozone. For example, the amplitude of the regional subsidence is greater than the local folding relief in the structural low of the syncline between the W-Gobi and Huoerguos anticlines, so the filling of the syncline trough is dominated by ancient slopes. There exist a row of subsurface anticline structures to the north of the Hutubi-Anjihai-Dushanzi anticline zone, named the N-Xihu-N-Dushanzi-W-Hutubi-N-Hutubi anticline zone in the western segment of the northern Tian Shan wedge top depozone
- (3) The transition between the trends of the stream morphology in the wedge top and foredeep depozones suggests the control of the structures of the foreland basin system on the trends in the stream morphology. All rivers, originating from the Tian Shan range and flowing north-north-eastward, are almost perpendicular to the range with relatively stable interval

lengths in the wedge top depozone, but divert to approximately parallel to the range in the foredeep depozone. Growth of anticlines in the front of the wedge-top depozone may have triggered a northward migration of the meandering channel of the Manas river in its lower reach

- (4) In the framework of the southern Junggar foreland basin system, changes in the sedimentation rates and the sedimentary environment in stratigraphic sections in the wedge top depozone may represent the forelandward migration of its depozone, rather than influence of regional tectonics or climate

Data Availability

The original seismic data supporting this research are owned by the China National Petroleum Corporation (CNPC) with commercial restrictions and are not accessible to the public or research community. The high-resolution seismic profiles used in this study can be accessed via: doi:10.6084/m9.figshare.19614342.v1.

Conflicts of Interest

The authors declare that they have no conflicts of interest.

Acknowledgments

This work was supported by the National Natural Science Foundation of China (grant numbers 42072153 and 42102250) and the Fundamental Research Funds for the Central Universities (grant number B200201025). China Scholarship Council (201806190214) provided financial support for Z. He for his research stay in Belgium.

References

- [1] P. Molnar and P. Tapponnier, "Cenozoic tectonics of Asia: effects of a continental collision: features of recent continental tectonics in Asia can be interpreted as results of the India-Eurasia collision," *Science*, vol. 189, no. 4201, pp. 419–426, 1975.
- [2] J. P. Avouac, P. Tapponnier, M. Bai, H. You, and G. Wang, "Active thrusting and folding along the northern Tien Shan and late Cenozoic Rotation of the Tarim relative to Dzungaria and Kazakhstan," *Journal of Geophysical Research-Solid Earth*, vol. 98, no. B4, pp. 6755–6804, 1993.
- [3] E. K. Dayem, P. Molnar, K. M. Clark, and A. Houseman, "Far-field lithospheric deformation in Tibet during continental collision," *Tectonics*, vol. 28, no. 6, 2009.
- [4] P. P. Huangfu, Z. H. Li, K. J. Zhang, W. M. Fan, J. M. Zhao, and Y. L. Shi, "India-Tarim lithospheric mantle collision beneath western Tibet controls the Cenozoic building of Tian Shan," *Geophysical Research Letters*, vol. 48, no. 14, 2021.
- [5] M. S. Hendrix, S. A. Graham, A. R. Carroll et al., "Sedimentary record and climatic implications of recurrent deformation in the Tian Shan: evidence from Mesozoic strata of the North Tarim, south Junggar, and Turpan basins, Northwest China," *Geological Society of America Bulletin*, vol. 104, no. 1, pp. 53–79, 1992.
- [6] S. Yang, J. Li, and Q. Wang, "The deformation pattern and fault rate in the Tianshan Mountains inferred from GPS observations," *Science in China Series D: Earth Sciences*, vol. 51, no. 8, pp. 1064–1080, 2008.
- [7] W. Yang, M. Jolivet, G. Dupont-Nivet, Z. J. Guo, Z. C. Zhang, and C. D. Wu, "Source to sink relations between the Tian Shan and Junggar Basin (Northwest China) from late Palaeozoic to quaternary: evidence from detrital U-Pb zircon geochronology," *Basin Research*, vol. 25, no. 2, pp. 219–240, 2013.
- [8] P. G. DeCelles and K. A. Giles, "Foreland basin systems," *Basin Research*, vol. 8, no. 2, pp. 105–123, 1996.
- [9] H. D. Sinclair, "Thrust wedge/foreland basin systems. Tectonics of sedimentary basins," in *Tectonics of Sedimentary Basins: Recent Advances*, C. Busby and A. Azor, Eds., pp. 522–537, Blackwell Publishing Ltd, 2012.
- [10] J. Sun, R. Zhu, and J. Bowler, "Timing of the Tianshan Mountains uplift constrained by magnetostratigraphic analysis of molasse deposits," *Earth and Planetary Science Letters*, vol. 219, no. 3-4, pp. 239–253, 2004.
- [11] J. Sun, Q. Xu, and B. Huang, "Late Cenozoic magnetostratigraphy and paleoenvironmental changes in the northern foreland basin of the Tian Shan Mountains," *Journal Geophysical Research*, vol. 112, no. B4, p. B04107, 2007.
- [12] J. Charreau, Y. Chen, S. Gilder et al., "Magnetostratigraphy and rock magnetism of the Neogene Kuitun He section (northwest China): implications for Late Cenozoic uplift of the Tianshan mountains," *Earth and Planetary Science Letters*, vol. 230, no. 1-2, pp. 177–192, 2005.
- [13] J. Charreau, Y. Chen, S. Gilder et al., "Neogene uplift of the Tian Shan Mountains observed in the magnetic record of the Jingou River section (Northwest China)," *Tectonics*, vol. 28, no. 2, 2009.
- [14] J. Ji, P. Luo, P. White, H. Jiang, L. Gao, and Z. Ding, "Episodic uplift of the Tianshan Mountains since the late Oligocene constrained by magnetostratigraphy of the Jingou River section, in the southern margin of the Junggar Basin, China," *Journal of Geophysical Research*, vol. 113, no. B5, article B05102, 2008.
- [15] J. Sun and Z. Zhang, "Syntectonic growth strata and implications for late Cenozoic tectonic uplift in the northern Tian Shan, China," *Tectonophysics*, vol. 463, no. 1-4, pp. 60–68, 2009.
- [16] H. H. Lu, D. W. Burbank, Y. L. Lin, and Y. M. Liu, "Late Cenozoic structural and stratigraphic evolution of the northern Chinese Tian Shan foreland," *Basin Research*, vol. 22, no. 3, pp. 249–269, 2010.
- [17] C. X. Li, G. Dupont-Nivet, and Z. Guo, "Magnetostratigraphy of the northern Tian Shan foreland, Taxi He section, China," *Basin Research*, vol. 23, no. 1, pp. 101–117, 2011.
- [18] M. Dubille and J. Lavé, "Rapid grain size coarsening at sandstone/conglomerate transition: similar expression in Himalayan modern rivers and Pliocene molasse deposits," *Basin Research*, vol. 27, no. 1, pp. 26–42, 2015.
- [19] J. Suppe, G. T. Chou, and S. C. Hook, "Rates of folding and faulting determined from growth strata," in *Thrust Tectonics*, K. R. McClay, Ed., pp. 05–121, Chapman and Hall, New York, NY, USA, 1992.
- [20] J. Poblet and K. McClay, "Geometry and kinematics of single layer detachment folds," *AAPG Bulletin*, vol. 80, no. 7, pp. 1085–1109, 1996.
- [21] S. Hardy, K. McClay, and J. Anton Muñoz, "Deformation and fault activity in space and time in high-resolution numerical

- models of doubly vergent thrust wedges," *Marine and Petroleum Geology*, vol. 26, no. 2, pp. 232–248, 2009.
- [22] Y. Song, *Geology of the Gas Accumulation Zone in the Junggar Basin*, Petroleum Industry Press, Beijing, China, 1995.
- [23] B. F. Windley, M. B. Allen, C. Zhang, Z. Y. Zhao, and G. R. Wang, "Paleozoic accretion and Cenozoic reformation of the Chinese Tien Shan range, Central Asia," *Geology*, vol. 18, no. 2, pp. 128–131, 1990.
- [24] J. Charvet, S. Laurent-Charvet, M. Faure, D. Cluzel, and K. D. Jong, "Palaeozoic tectonic evolution of the Tianshan belt, NW China," *Science China: Earth Sciences*, vol. 54, no. 2, pp. 166–184, 2011.
- [25] W. Xiao, B. F. Windley, M. B. Allen, and C. Han, "Paleozoic multiple accretionary and collisional tectonics of the Chinese Tianshan orogenic collage," *Gondwana Research*, vol. 23, no. 4, pp. 1316–1341, 2013.
- [26] T. A. Dumitru, D. Zhou, E. Z. Chang et al., "Uplift, exhumation, and deformation in the Chinese Tian Shan," in *Paleozoic and Mesozoic Tectonic Evolution of Central Asia: from Continental Assembly to Intracontinental Deformation*, M. S. Hendrix and G. A. Davis, Eds., pp. 71–99, Geological Society of America Memoir, 2001.
- [27] J. De Grave, S. Glorie, M. M. Buslov et al., "The thermotectonic history of the Song-Kul Plateau, Kyrgyz Tien Shan: constraints by apatite and titanite thermochronometry and zircon U/Pb dating," *Gondwana Research*, vol. 20, no. 4, pp. 745–763, 2011.
- [28] S. Glorie, J. De Grave, M. M. Buslov et al., "Tectonic history of the Kyrgyz South Tien Shan (Atbashi-Inylchek) suture zone: the role of inherited structures during deformation-propagation," *Tectonics*, vol. 30, no. 6, article TC6016, 2011.
- [29] E. A. Macaulay, E. R. Sobel, A. Mikolaichuk, A. Landgraf, B. Kohn, and F. Stuart, "Thermochronologic insight into late Cenozoic deformation in the basement-cored Terskey Range, Kyrgyz Tien Shan," *Tectonics*, vol. 32, no. 3, pp. 487–500, 2013.
- [30] G. Jepson, S. Glorie, D. Konopelko et al., "Low temperature thermochronology of the Chatkal-Kurama terrane (Uzbekistan-Tajikistan): insights into the Meso-Cenozoic thermal history of the western Tian Shan," *Tectonics*, vol. 37, no. 10, pp. 3954–3969, 2018.
- [31] Z. Y. He, B. Wang, S. Glorie et al., "Mesozoic building of the Eastern Tianshan and East Junggar (NW China) revealed by low-temperature thermochronology," *Gondwana Research*, vol. 103, pp. 37–53, 2022.
- [32] A. Yin, S. Nie, P. Craig et al., "Late Cenozoic tectonic evolution of the southern Chinese Tian Shan," *Tectonics*, vol. 17, no. 1, pp. 1–27, 1998.
- [33] E. R. Sobel, J. Chen, and R. V. Heermance, "Late Oligocene–Early Miocene initiation of shortening in the Southwestern Chinese Tian Shan: Implications for Neogene shortening rate variations," *Earth and Planetary Science Letters*, vol. 247, no. 1–2, pp. 70–81, 2006.
- [34] M. Jolivet, S. Dominguez, J. Charreau, Y. Chen, Y. Li, and Q. Wang, "Mesozoic and Cenozoic tectonic history of the central Chinese Tian Shan: reactivated tectonic structures and active deformation," *Tectonics*, vol. 29, no. 6, article TC6019, 2010.
- [35] B. Fu, A. Lin, K. Kano, T. Maruyama, and J. Guo, "Quaternary folding of the eastern Tian Shan, Northwest China," *Tectonophysics*, vol. 369, no. 1–2, pp. 79–101, 2003.
- [36] C. Li, S. L. Wang, M. Naylor, H. Sinclair, and L. S. Wang, "Evolution of the Cenozoic Tarim Basin by flexural subsidence and sediment ponding: insights from quantitative basin modelling," *Marine and Petroleum Geology*, vol. 112, article 104047, 2020.
- [37] Q. Wang, P. Z. Zhang, J. T. Freymueller et al., "Present-day crustal deformation in China constrained by global positioning system measurements," *Science*, vol. 294, no. 5542, pp. 574–577, 2001.
- [38] A. V. Zubovich, X. Q. Wang, Y. G. Scherba et al., "GPS velocity field for the Tien Shan and surrounding regions," *Tectonics*, vol. 29, no. 6, article TC6014, 2010.
- [39] M. B. Allen, B. F. Windley, and Z. Chi, "Active alluvial systems in the Korla basin, Tien Shan, Northwest China: sedimentation in a complex foreland basin," *Geological Magazine*, vol. 128, no. 6, pp. 661–666, 1991.
- [40] Q. Deng, X. Feng, P. Zhang, X. Xu, X. Yang, and S. Peng, "Paleoseismology of the northern piedmont of Tianshan Mountains, northwestern China," *Journal of Geophysical Research*, vol. 101, no. B3, pp. 5895–5920, 1996.
- [41] H. F. Lu, S. L. Wang, and C. Jia, "The mechanism of the southern Junggar Cenozoic thrusts," *Earth Sciences Frontiers*, vol. 14, no. 4, pp. 168–174, 2007.
- [42] BGMRX (Bureau of Geological and Mineral Resources of BGMRX the Xinjiang Uygur Autonomous Region), *Regional geology of Xinjiang Uygur Autonomous region, People's Republic of China Ministry of Geology and Mineral Resources*, p. 841, Geological Publishing House, Beijing, 1993.
- [43] W. H. Bian, J. Hornung, Z. H. Liu, P. J. Wang, and M. Hinderer, "Sedimentary and palaeoenvironmental evolution of the Junggar Basin, Xinjiang, Northwest China," *Palaeo-bio Palaeoenv*, vol. 90, no. 3, pp. 175–186, 2010.
- [44] B. C. Burchfiel, E. T. Brown, D. Qidong et al., "Crustal shortening on the margins of the Tien Shan, Xinjiang, China," *International Geology Review*, vol. 41, no. 8, pp. 665–700, 1999.
- [45] M. S. Hendrix, T. A. Dumitru, and S. A. Graham, "Late Oligocene-early Miocene unroofing in the Chinese Tian Shan: an early effect of the India-Asia collision," *Geology*, vol. 22, no. 6, pp. 487–490, 1994.
- [46] S. L. Wang, Y. Chen, J. Charreau, D. T. Wei, and D. Jia, "Tectono-stratigraphic history of the southern Junggar basin: seismic profiling evidences," *Terra Nova*, vol. 25, no. 6, pp. 490–495, 2013.
- [47] M. E. Bullen, D. W. Burbank, J. I. Garver, and K. Y. Abdrakhmatov, "Late Cenozoic tectonic evolution of the northwestern Tien Shan: new age estimates for the initiation of mountain building," *Geological Society of America Bulletin*, vol. 113, no. 12, pp. 1544–1559, 2001.
- [48] S. Guan, J. M. Stockmeyer, J. H. Shaw, A. Plesch, and J. Zhang, "Structural inversion, imbricate wedging, and out-of-sequence thrusting in the southern Junggar fold-and-thrust belt, northern Tian Shan, China," *AAPG Bulletin*, vol. 100, no. 9, pp. 1443–1468, 2016.
- [49] J. M. Stockmeyer, J. H. Shaw, and S. Guan, "Seismic hazards of multisegment thrust-fault ruptures: insights from the 1906 Mw 7.4–8.2 Manas, China, earthquake," *Seismological Research Letters*, vol. 85, no. 4, pp. 801–808, 2014.
- [50] J. H. Qiu, G. Rao, X. Wang, D. S. Yang, and L. X. Xiao, "Effects of fault slip distribution on the geometry and kinematics of the southern Junggar fold-and-thrust belt, northern Tian Shan," *Tectonophysics*, vol. 772, article 228209, 2019.

- [51] S. L. Wang, Y. Chen, and H. F. Lu, "Growth of the Huoerguosi anticline (the North Tian Shan Mountains) by limb rotation since the late Miocene," *Chinese Science Bulletin*, vol. 53, pp. 3028–3036, 2008.
- [52] H. H. Lu, D. J. Li, D. Y. Wu et al., "Spatiotemporal patterns of the late quaternary deformation across the northern Chinese Tian Shan foreland," *Earth-Science Reviews*, vol. 194, pp. 19–37, 2019.
- [53] Y. Wang, D. Jia, H. Zhang et al., "Spatial and temporal associations of traps and sources: insights into exploration in the southern Junggar foreland basin, northwestern China," *Journal of Asian Earth Sciences*, vol. 198, article 104078, 2019.
- [54] Y. J. Wang, D. Jia, J. G. Pan et al., "Multiple-phase tectonic superposition and reworking in the Junggar Basin of northwestern China—implications for deep-seated petroleum exploration," *AAPG Bulletin*, vol. 102, no. 8, pp. 1489–1521, 2018.
- [55] C. Li, S. L. Wang, Y. X. Li et al., "Growth of the Tian Shan drives migration of the conglomerate-sandstone transition in the southern Junggar Foreland Basin," *Geophysical Research Letters*, vol. 49, no. 4, 2022.
- [56] C. L. Malatesta and J. P. Avouac, "Contrasting river incision in north and South Tian Shan piedmonts due to variable glacial imprint in mountain valleys," *Geology*, vol. 46, no. 7, pp. 659–662, 2018.
- [57] B. L. Yu, W. H. Liu, X. L. Liu et al., "Controlling factor and concentration rule of Neogene reservoir genesis in Chepaizi area of Junggar basin," *Oil Geophysical Prospecting*, vol. 43, pp. 45–53, 2008.
- [58] J. Charreau, J. P. Avouac, Y. Chen, S. Dominguez, and S. Gilder, "Miocene to present kinematics of fault-bend folding across the Huerguosi anticline, northern Tianshan (China), derived from structural, seismic, and magnetostratigraphic data," *Geology*, vol. 36, no. 11, pp. 871–874, 2008.
- [59] J. Charreau, M. L. Kent-Corson, L. Barrier et al., "A high-resolution stable isotopic record from the Junggar Basin (NW China): implications for the paleotopographic evolution of the Tianshan Mountains," *Earth and Planetary Science Letters*, vol. 341–344, pp. 158–169, 2012.
- [60] J. Jackson, R. Van Dissen, and K. Berryman, "Tilting of active folds and faults in the Manawatu region, New Zealand: evidence from surface drainage patterns," *New Zealand Journal of Geology and Geophysics*, vol. 41, no. 4, pp. 377–385, 1998.
- [61] C. R. Twidale, "River patterns and their meaning," *Earth-Science Review*, vol. 67, no. 3–4, pp. 159–218, 2004.
- [62] H. H. Lu, D. Y. Wu, L. Cheng et al., "Late quaternary drainage evolution in response to fold growth in the northern Chinese Tian Shan foreland," *Geomorphology*, vol. 299, pp. 12–23, 2017.
- [63] H. H. Lu, L. Cheng, Z. Wang et al., "Latest quaternary rapid river incision across an inactive fold in the northern Chinese Tian Shan foreland," *Quaternary Science Reviews*, vol. 179, pp. 167–181, 2018.
- [64] C. L. Malatesta, J. P. Avouac, D. N. Brown et al., "Lag and mixing during sediment transfer across the Tian Shan piedmont caused by climate-driven aggradation-incision cycles," *Basin Research*, vol. 30, no. 4, pp. 613–635, 2018.
- [65] L. Zhang and Y. Li, "On the changes of Manas Lake in the past 300 year," *Collections of Essays on Chinese Historical Geography*, vol. 19, pp. 127–142, 2004.
- [66] L. Zhang, G. Han, and D. Yan, "Changes of Santun River and Hutubi River (Xinjiang, China) in the past 300 years," *Acta Scientiarum Naturalium Universitatis Pekinensis*, vol. 40, pp. 957–970, 2004.
- [67] W. G. Cui, G. J. Mu, H. Wang, and N. N. Ma, "Evolution of the lower reaches of the Manas river based on information from remote sensing images," *Advances in Earth Science*, vol. 22, no. 3, pp. 7–13, 2007.
- [68] J. Suppe and D. A. Medwedeff, "Geometry and kinematics of fault-propagation folding," *Eclogae Geologicae Helvetiae*, vol. 83, pp. 409–454, 1990.
- [69] S. Bernard, J. P. Avouac, S. Dominguez, and M. Simoes, "Kinematics of fault-related folding derived from a sandbox experiment," *Journal of Geophysical Research*, vol. 112, no. B3, article B03S12, 2007.
- [70] B. L. Li, S. W. Guan, Z. X. Chen et al., *Fault-Related Fold Theory and Application: Case Study on the Structural Geology in the Southern Junggar Basin*, Petroleum Industry Press, 2010.
- [71] P. B. Flemings and T. E. Jordan, "A synthetic stratigraphic model of Foreland Basin development," *Journal of Geophysical Research-Solid Earth*, vol. 94, no. B4, pp. 3851–3866, 1989.
- [72] H. D. Sinclair, B. J. Coakley, P. A. Allen, and A. B. Watts, "Simulation of foreland basin stratigraphy using a diffusion model of mountain belt uplift and erosion: an example from the Central Alps, Switzerland," *Tectonics*, vol. 10, no. 3, pp. 599–620, 1991.
- [73] P. G. DeCelles and P. C. DeCelles, "Rates of shortening, propagation, underthrusting, and flexural wave migration in continental orogenic systems," *Geology*, vol. 29, no. 2, pp. 135–138, 2001.
- [74] M. Naylor and H. D. Sinclair, "Pro- vs. retro-foreland basins," *Basin Research*, vol. 20, no. 3, pp. 285–303, 2008.
- [75] C. Li, S. L. Wang, and L. S. Wang, "Tectonostratigraphic history of the southern Tian Shan, western China, from seismic reflection profiling," *Journal of Asian Earth Sciences*, vol. 172, pp. 101–114, 2019.
- [76] S. L. Wang, Y. Chen, J. Charreau et al., "Underthrusting of the Tarim lithosphere beneath the Western Kunlun range, insights from seismic profiling evidence," *Tectonics*, vol. 40, 2021.
- [77] B. K. Horton and P. G. DeCelles, "The modern foreland basin system adjacent to the Central Andes," *Geology*, vol. 25, no. 10, pp. 895–898, 1997.
- [78] H. Lyon-Caen and P. Molnar, "Gravity anomalies, flexure of the Indian Plate, and the structure, support and evolution of the Himalaya and Ganga Basin," *Tectonics*, vol. 4, no. 6, pp. 513–538, 1985.
- [79] H. D. Sinclair and P. A. Allen, "Vertical versus horizontal motions in the alpine orogenic wedge: stratigraphic response in the foreland basin," *Basin Research*, vol. 4, no. 3–4, pp. 215–232, 1992.
- [80] M. Simoes and J. P. Avouac, "Investigating the kinematics of mountain building in Taiwan from the spatiotemporal evolution of the foreland basin and western foothills," *Journal of Geophysical Research*, vol. 111, no. B10, article B10401, 2006.
- [81] E. V. Burov, M. G. Kogan, H. Lyon-Caen, and P. Molnar, "Gravity anomalies, the deep structure, and dynamic processes beneath the Tien Shan," *Earth and Planetary Letters*, vol. 96, no. 3–4, pp. 367–383, 1990.
- [82] X. D. Jiang, "Dynamic support of the Tien Shan lithosphere based on flexural and rheological modeling," *Journal of Asian Earth Sciences*, vol. 93, pp. 37–48, 2014.

- [83] M. Daeron, J. P. Avouac, and J. Charreau, "Modeling the shortening history of a fault tip fold using structural and geomorphic records of deformation," *Journal of Geophysical Research*, vol. 112, no. B3, article B03S13, 2007.
- [84] C. Y. Wu, G. D. Wu, J. Shen, X. Y. Dai, J. B. Chen, and H. P. Song, "Late Quaternary tectonic activity and crustal shortening rate of the Bogda mountain area, eastern Tian Shan, China," *Journal of Asian Earth Sciences*, vol. 119, pp. 20–29, 2016.